

## Research Article

# Reconstruction of Cardiac Cine MR Images from Partial $k$ -Space

Josiane Yankam Njiwa,<sup>1</sup> Yuemin Zhu,<sup>1</sup> Jianhua Luo,<sup>2</sup> and Bassem Hiba<sup>3</sup>

<sup>1</sup>CREATIS, CNRS UMR5520 & INSERM U630, INSA Lyon, UCB Lyon, University of Lyon, 69621 Villeurbanne, France

<sup>2</sup>College of Life Science and Technology, Shanghai Jiaotong University, 200240 Shanghai, China

<sup>3</sup>Magnetic Resonance Center, CNRS-Victor Segalen University of Bordeaux 2, 33076 Bordeaux, France

Correspondence should be addressed to Josiane Yankam Njiwa, joad24@yahoo.com

Received 8 January 2010; Revised 17 March 2010; Accepted 7 April 2010

Copyright © 2010 Josiane Yankam Njiwa et al. This is an open access article distributed under the Creative Commons Attribution License, which permits unrestricted use, distribution, and reproduction in any medium, provided the original work is properly cited.

Short acquisition time is essential in cardiac cine magnetic resonance imaging (MRI), in particular for sick patients who have difficulties to hold their breath. This paper investigates the use of two reconstruction methods, initially proposed for static images, for reconstructing cardiac cine images from partial  $k$ -space. A new acquisition schema which makes use of temporal redundancies within data is proposed. The results show that, in comparison with the full  $k$ -space acquisition, the acquisition time can be reduced by a factor of 4 while obtaining a good reconstruction quality.

## 1. Introduction

Magnetic resonance cine imaging allows noninvasive determination of morphologic and functional parameters of the heart. Generally, breath-hold cine sequences are used for exclusion of artifacts caused by respiratory motion. Due to the limited acquisition time, a compromise has to be found between spatial and temporal resolution on one hand and the duration of the breath hold on the other hand. In conventional Fourier magnetic resonance imaging, reduction of the data acquisition time  $T_{\text{acq}}$  can be achieved by acting on the repetition time  $T_R$ , the number of phase encodings  $N_{\text{enc}}$ , or the number of signal acquisition (signal averaging)  $N_{\text{acc}}$  for each encoded signal, individually or simultaneously, according to the following expression  $T_{\text{acq}} = N_{\text{acc}} N_{\text{enc}} T_R$ . It is nevertheless worth to notice that for imaging scheme where data acquisition speed is crucial enough for the method under consideration, no averaging should be performed, thus  $N_{\text{acc}} = 1$ . The present work deals with reducing  $N_{\text{enc}}$  (reduction of the spatial resolution), which leads to partial  $k$ -space acquisition. Spatial image reconstruction from partial  $k$ -space exhibits in general two main drawbacks: (a) Loss of spatial resolution and (b) Image artifacts such as Gibbs ringing or image aliasing.

Over the years, a number of partial  $k$ -space strategies have been proposed to avoid drawbacks encountered when reconstructing static magnetic resonance (MR) images [1–8]. These techniques have been used for dynamic imaging as

well. In an attempt to further increase the acquisition rate by reducing the amount of acquired data by a given factor, referred to as the reduction factor, several methods dedicated to dynamic MR images reconstruction have been reported in the literature [9–15]. Even though parallel imaging is commonly used to acquire cine MRI, few reconstruction methods have been proposed for reconstructing cardiac cine images [16]. Relatively fewer methods are available for cardiac cine images reconstruction from partial  $k$ -space [16–20], compared to the body of literature on static image reconstruction. For example, the keyhole method initially proposed for general dynamic imaging is not suitable for reconstructing cardiac cine images without priors such as the direction of the left ventricle motion [17]. To overcome the limitations of such reconstruction methods due to large motion, we will investigate, on one hand, the capabilities of the Homodyne detection (HM) and the Projection onto Convex Set (POCS) reconstruction methods, initially proposed for static images, for reconstructing frame by frame cardiac cine images from partially sampled  $k$ -space, using only correlations in  $k$ -space. The approach proposed in [11] is a dynamic POCS reconstruction algorithm, based on the concepts of image recovery theory which approximately double the temporal resolution. This algorithm requires acquisition of a fully sampled precontrast image, which is prior to contrast agent administration, to fill the void of high spatial frequencies occurring in half-Fourier data acquisition. To further reduce the acquisition time of cardiac

cine data is proposed, on the other hand, a modified version of the keyhole acquisition schema. The proposed method exploits both temporal correlations between image series and data substitution in  $k$ -space to perform reconstruction of cardiac cine images. Prior to the acquisition of the dynamic image series, two asymmetric partially sampled baseline images were acquired, one corresponding to the diastolic phase and the other to the systolic phase. Then in an attempt of reducing cine data acquisition time, the proposed approach relies on the principle of acquiring only the symmetric low-frequency part of the  $k$ -space data, and updating the missing high spatial frequencies of the image series as illustrated in Figure 1(d), depending on whether it is the diastolic or systolic phase of the cardiac cycle. Finally, each formed  $k$ -space dataset is reconstructed separately using the HM and POCS reconstruction techniques. Reduction of the acquisition time by a factor of up to 4 can be achieved using the abovementioned reconstruction techniques.

## 2. Materials and Methods

**2.1. Homodyne Detection Approach (HM).** Homodyne detection approach (HM) [1] is based on the fact that a fully sampled noiseless  $k$ -space can be represented by its low and high spatial frequencies. So, the partial  $k$ -space depicted in Figure 1(a), for example, is viewed as the superposition of the entire low frequencies and only one half of the high spatial frequencies. To compensate for having only one half of the high-frequency components, those high spatial frequencies are doubled. One crucial point of this method concerns the step of phase estimation. The low frequencies are used to estimate the phase  $\hat{\varphi}(x, y)$  of the entire image, by assuming that the phase image is a slowly varying one and can then be represented by the phase corresponding to low spatial frequencies. Once  $\hat{\varphi}(x, y)$  is estimated, the next step is to find an image function which satisfies both the measured data  $S(k_x, k_y)$  and the phase constraint  $\hat{\varphi}(x, y)$ . A weighting function can be used to smooth the sharp transitions between the zeros padded and the measured data and to counter the imbalance between the low- and high-frequency data due to the lack of negative high frequencies. The inverse Fourier Transform is applied to the weighted dataset and the obtained image is phase corrected. The desired reconstructed image corresponds to the real part of this phase corrected image.

**2.2. Projection Onto Convex Set Approach.** The POCS method [2–4] is an iterative approach based on the principle that the desired image is the intersection of all images whose Fourier transform agrees with the measured partial data and all images whose phase is the same as the phase estimate. The phase shifting is estimated using central  $k$ -space data, and the iterative process of image reconstruction can be written as follows:

$$I_{m+1} = P_1 P_2 \{I_m\}, \quad (1)$$

where  $I_{m+1}$  is the current image and  $P_1$  and  $P_2$  are the two operators such as

$$P_1(I(x, y)) = |I(x, y)| e^{i\hat{\varphi}(x, y)}, \quad (2)$$

where  $\hat{\varphi}(x, y)$  is the estimated phase, and

$$P_2(I(x, y)) = T^{-1} R T \{I(x, y)\}, \quad (3)$$

where  $T$  is the Fourier transform operator,  $T^{-1}$  the inverse Fourier transform operator and  $R$  the data replacement operator defined as follows:

$$R\{\hat{S}(k_x, k_y)\} = \begin{cases} S(k_x, k_y), & -k_{y_l} \leq k_y \leq \frac{N}{2} - 1, \\ \hat{S}(k_x, k_y) & \text{otherwise} \end{cases} \quad (4)$$

with  $N$  being the total number of phase encoding lines.

**2.3. Data Acquisition.** The  $k$ -space cine data were acquired on a clinical 1.5T whole-body Siemens Sonata system (Erlangen, Germany). A segmented TRUE FISP sequence was used to acquire ECG-gated cardiac cine images in short and long-axis orientations of the heart. Data were carried out at the CERMEP center in Lyon, France, and 3 patients were imaged in this study.

For a cardiac cine sequence of  $256 \times 176$  pixels, 22 frames per cardiac cycle, and 11 phase encoding lines per segment, 16 cardiac cycles were necessary to achieve a full  $k$ -space against 10 cardiac cycles for a 5/8 of the  $k$ -space and 4 cardiac cycles for a 1/4 of the  $k$ -space.

**2.4. Temporal Correlations.** To achieve image reconstruction with an acquisition reduction factor of 4, we introduce the use of temporal redundancies into the HM and POCS reconstruction processes. The thus obtained reconstruction scheme is illustrated in Figure 1, in which the first line shows the  $k$ -space sampling coverage of the used baseline datasets. The second line of Figure 1 illustrates the dynamic acquisition stage of  $k$ -space data (only the symmetric low spatial frequencies are acquired) and the last line represents the reconstructed  $k$ -space datasets. Two asymmetric partially sampled  $k$ -space baseline datasets are first acquired, as depicted in Figures 1(a) and 1(b), one corresponds to the baseline diastolic (denoted by BD) phase and the other to the baseline systolic (denoted by BS) phase. Then, to shorten the acquisition time, a reduced number of phase encoding lines (central  $k$ -space frequencies) is acquired for each frame composing the temporal image series (Figure 1(c)), thus reducing the number of cardiac cycles needed for a conventional acquisition (Figure 1(a) or Figure 1(b)). Once the data are acquired, the low spatial frequencies of the dynamic image series are substituted to the corresponding baseline dataset, Figure 1(a) for the diastolic phase and Figure 1(b) for the systolic phase, as shown in Figure 1(d) to form the conventional  $k$ -space coverage required for enabling the HM and POCS reconstruction techniques to be applied. Finally, each spatial frame of the cine cardiac sequence is reconstructed independently from the thus obtained  $k$ -space data using both techniques.

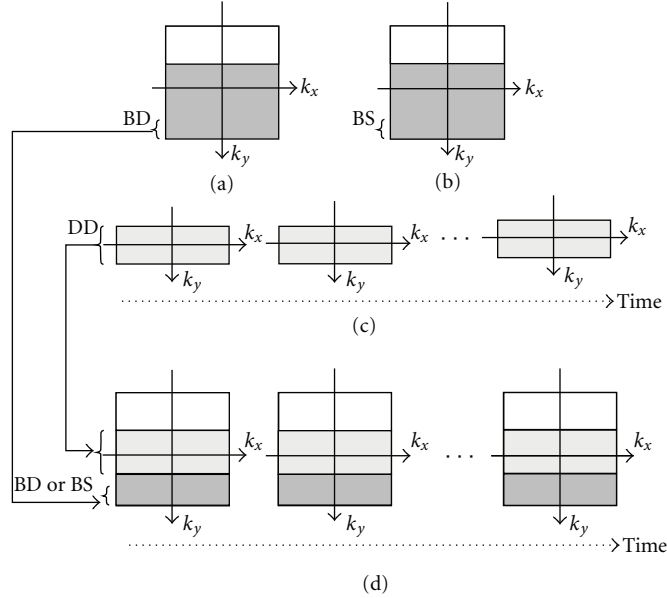


FIGURE 1:  $K$ -space sampling: typical partial  $k$ -space sampling coverage representing the baseline datasets of (a) Baseline diastolic phase (BD) and (b) baseline systolic phase (BS) of the cardiac cycle, (c) dynamic acquisition of  $k$ -space center (DD), only 25% of raw data are acquired. The gray part represents the acquired data, (b) 25% of  $k$ -space data are acquired for each time frame, (d) low spatial frequencies of the dynamic data are merged with the baseline high spatial frequencies, depending on the phase in the cardiac cycle, to form the optimal reconstruction dataset series for the methods under comparison.

2.5. *Quantitative Analysis.* The reconstruction quality was assessed both qualitatively and quantitatively. For qualitative evaluation, we computed the difference image between the image reconstructed from the full  $k$ -space and that reconstructed from partial  $k$ -space, in a region around the heart since the HM-reconstruction method presents large errors outside the heart which are of minor interest. For quantitative evaluation, we used the normalized mean squared error (NMSE), in the same region, defined by

$$\text{NMSE} = \frac{1}{PQ} \sum \sum \frac{(I(x, y) - I_R(x, y))^2}{\bar{I}(x, y) \cdot \bar{I}_R(x, y)}, \quad (5)$$

where  $I(x, y)$  is the image reconstructed from the full  $k$ -space,  $I_R(x, y)$  the image reconstructed from partial  $k$ -space using the HM or POCS method,  $P$  and  $Q$  are the sizes of the ROIs.

We computed the mean deviation between the error values obtained using, respectively, 5/8 and 1/4 of the complete  $k$ -space data. The mean deviation is defined by

$$\text{MD} = \frac{1}{l} \sum |E - \bar{E}|, \quad (6)$$

where  $l$  is twice the number of frames in the temporal sequence,  $E$  the error values (NMSE), and  $\bar{E}$  the mean error value.

The signal-to-noise ratio (SNR) and the contrast-to-noise ratio (CNR) were also used for quantitatively evaluating the reconstruction quality. These two criteria were assessed according to [20]: three separate regions of interest (ROIs) are defined in each frame of each cine sequence. The first ROI is in the blood pool, the second in the

left ventricular myocardium, and the last in the image background, which is assimilated to the noise. The blood SNR ( $\text{SNR}_{\text{Blood}}$ ) is calculated as

$$\text{SNR}_{\text{Blood}} = \frac{\text{SI}_{\text{Blood}}}{\text{SD}_{\text{Noise}}}, \quad (7)$$

where  $\text{SI}_{\text{Blood}}$  is the mean value of the signal intensity measured in the blood pool, and  $\text{SD}_{\text{Noise}}$  the standard deviation of the noise.

The myocardium SNR ( $\text{SNR}_{\text{Myocardium}}$ ) is computed as

$$\text{SNR}_{\text{Myocardium}} = \frac{\text{SI}_{\text{Myocardium}}}{\text{SD}_{\text{Noise}}}, \quad (8)$$

where  $\text{SI}_{\text{Myocardium}}$  is the mean value of the signal intensity measured in the left ventricular myocardium.

The blood-to-myocardium tissue CNR is defined by

$$\text{CNR} = \frac{\text{SI}_{\text{Blood}} - \text{SI}_{\text{Myocardium}}}{\text{SD}_{\text{Noise}}}. \quad (9)$$

Six cardiac cine image series (end diastolic frames) were used from the available datasets for quantitative analysis of the HM, POCS and the full  $k$ -space reconstruction techniques. Four series of  $t$ -tests were performed to compare the results of quantitative and visual image quality evaluations. The first  $t$ -test was performed between the full  $k$ -space and HM-reconstructed image values, while the second was between the full  $k$ -space and HM-reconstructed image values using 25% of the full  $k$ -space data (HM\_1/4). The third  $t$ -test was performed between the full  $k$ -space and POCS-reconstructed image values, while the fourth was

TABLE 1: NMSE error values computed for the reconstructed images shown on Figure 2.

	HM	HM_1/4	POCS	POCS_1/4
Patient 1	0.0935	0.0973	0.0030	0.0041
Patient 2	0.0805	0.1419	0.0032	0.0102
Patient 3	0.1382	0.1240	0.0030	0.0049

between the full  $k$ -space and POCS-reconstructed image values using 25% of the entire  $k$ -space data (POCS\_1/4).  $P$ -values were then computed with respect to the full  $k$ -space reconstruction results;  $P < .05$  means that the differences are significant between the full  $k$ -space image and the partial  $k$ -space reconstructed ones.

### 3. Results

Figure 2 illustrates the results of reconstructing short-axis cardiac cine image series, from the three imaged patients, with the conventional constrained reconstruction methods (HM and POCS) and with the proposed acquisition schemas (HM\_1/4 and POCS\_1/4). All the time frames are zoomed to the heart. This figure also shows a qualitative comparison between the images reconstructed with the HM and POCS techniques using 5/8 and 1/4 of the full  $k$ -space data. The results are additionally compared to the complete  $k$ -space reconstructed images. It is observed that both HM and POCS methods allow reconstructing cardiac cine images and to a large extent, the image quality obtained with the proposed acquisition schema looked very similar to those obtained with the conventional reconstruction methods using 5/8 of the full  $k$ -space data. However, the HM and POCS methods did not lead to exactly the same results. The quality of the image reconstructed using the POCS method is closer to that of the full  $k$ -space reference image both when using 5/8 of the  $k$ -space data, and exploiting only  $k$ -space redundancies within data, and when using 1/4 of the raw data, associated to the use of both  $k$ -space and temporal correlations, for the reconstruction. In contrast, with the HM technique, the reconstructed images lose the dynamic range in comparison with that of the reference images, but preserve nevertheless essential characteristics of the latter. The POCS reconstruction technique achieved the lowest error values as shown in Table 1.

Figure 3 presents the error (NMSE) values for a complete cardiac cine sequence. We can observe that, although being qualitatively similar, the images reconstructed with 1/4 of the full  $k$ -space data (exploiting both  $k$ -space and temporal redundancies) using both methods present slightly greater error values than those reconstructed with 5/8 of the entire  $k$ -space data (exploiting only  $k$ -space correlations). However, in the systolic phase, the error values computed with HM\_1\_4 are smaller than those computed with the conventional HM. This is due to large motion present in the systolic phase. We can also note that, the worst images, qualitatively and quantitatively meaning, are reconstructed with the HM method.

The mean deviation for the POCS technique is  $MD = 0.34\%$  whereas for the HM technique it is  $MD = 0.86\%$ . So, the error values computed when using 5/8 of the  $k$ -space data, and exploiting  $k$ -space correlations, have appreciably the same behavior as those computed acquiring only 25%, using both  $k$ -space and temporal correlations, of the  $k$ -space data and using the POCS method whereas the dispersion in the given datasets is higher.

Table 2 shows mean  $\pm$  SD values for  $SNR_{Blood}$ ,  $SNR_{Myocardium}$  and CNR. The  $t$ -tests show that the POCS reconstruction technique resulted in larger  $SNR_{Blood}$  and  $SNR_{Myocardium}$  values than the HM technique. The values obtained by the POCS are close to those obtained by the full  $k$ -space reconstruction one according to the  $P$  values whereas the HM method gives results which present significant differences with the full  $k$ -space results. Table 2 also illustrates that, when acquiring 25% of  $k$ -space data and using temporal redundancies for the reconstruction, POCS allows a reconstruction quality which is much similar to the full  $k$ -space reconstruction one according to the  $P$  values whereas the HM method gives results which present significant differences with the full  $k$ -space results. The lack of high spatial frequencies reduces the noise level in  $k$ -space data, which could be at the origin of the slightly higher SNR and CNR values compared with those computed in the full  $k$ -space reconstructed images.

### 4. Discussion

We have proposed a new method for reconstructing cardiac cine images from partial  $k$ -space. The method is based on introducing temporal correlation into the HM and POCS reconstruction processes. The results show that, without using any temporal correlation, and using only  $k$ -space correlations, an acceptable reconstruction quality can be obtained with a time reduction factor of about 2. In contrast, when exploiting both temporal and  $k$ -space redundancies, a time reduction factor of 4 can be achieved for cardiac cine image sequences while maintaining an acceptable image quality. The images reconstructed in this case are similar to those reconstructed with the full  $k$ -space data especially in the case when using the POCS-reconstructed method. Furthermore, for the same reconstruction scheme, the POCS method yields better results than the HM method in terms of both qualitative and quantitative criteria. The reason is likely that the HM method is more sensitive to the accuracy of phase estimation and motion compared to the POCS method that compensates for inaccurate phase estimation by an iterative process updating missing  $k$ -space data. The capabilities of POCS approach can be further extended by considering time as a sampling axis in the same fashion as for the phase encoding axes. In this way, the acquisition in both space and time can be balanced to decrease the acquisition time. An important aspect of the proposed approaches is the way high-frequency missed data are recovered. In this way, a better use of the temporal correlations between  $k$ -space data is made. Another important point is the fact that it is unnecessary to make assumptions about the signal distribution and at the same time, it does not overconstrain



FIGURE 2: Results from three patients using the conventional HM method (HM), the proposed HM method (HM\_1/4), the conventional POCS method (POCS), and the proposed POCS method (POCS\_1/4), respectively, (b), (d), and (f) are images corresponding to the difference between the full  $k$ -space reconstructed image and the partial  $k$ -space reconstructed images.

TABLE 2: Mean  $\pm$  standard deviation values of SNR and CNR measured in the full  $k$ -space HM- and POCS-reconstructed images, respectively. In the brackets are inscribed the  $P$  values which represent the values of the  $t$ -test between the full  $k$ -space and the partial  $k$ -space reconstructed images. HM and POCS represent the conventional HM and POCS reconstruction methods. HM\_1/4 and POCS\_1/4 represent the proposed reconstruction approaches.

	SNR <sub>Blood</sub>	SNR <sub>Myocardium</sub>	CNR
Full $k$ -space	$36.4 \pm 6.32$	$8.72 \pm 1.36$	$27.7 \pm 5.68$
HM	$17.8 \pm 2.66$ (0.0001)	$4.09 \pm 0.76$ (0.00009)	$13.7$ (0.0002)
HM_1/4	$17.2 \pm 3.24$ (0.00001)	$4.19 \pm 0.63$ (0.00001)	$13 \pm 2.88$ (0.00003)
POCS	$37.2 \pm 9.05$ (0.86)	$9.18 \pm 3.12$ (0.65)	$28.1 \pm 6.32$ (0.92)
POCS_1/4	$37.3 \pm 10.82$ (0.58)	$9.77 \pm 3.02$ (0.31)	$27.6 \pm 7.98$ (0.68)

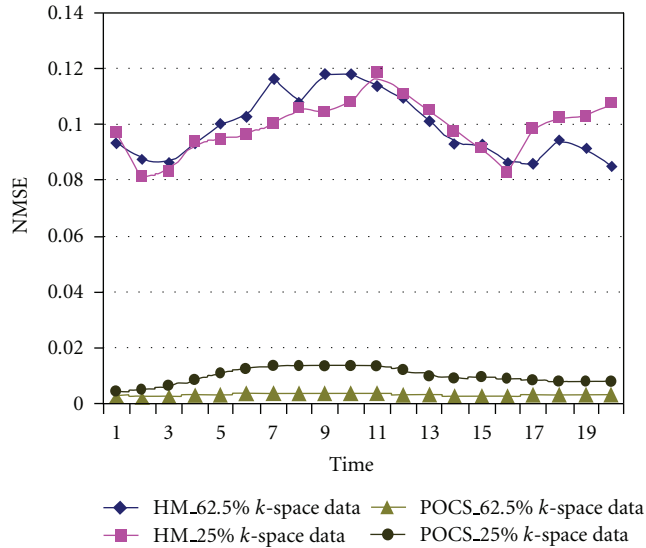


FIGURE 3: NMSE curves corresponding to the reconstructions using 5/8 and 1/4 of  $k$ -space data. These values are calculated for a full cardiac cine sequence.

the reconstruction algorithm. One limit of the method is that if the reduction factor is increased excessively, the phase estimate will be poor and image artifacts may occur in the reconstructed images.

In this study, the cardiac cycle was arbitrary divided in the diastolic and systolic phases and the baseline images were acquired during 10 cardiac cycles as explained in the text above. In view of the results obtained, it would be possible to acquire only the high spatial frequencies of the baseline images (3/8 of the full  $k$ -space data corresponding to an acquisition time of 264 ms) achievable in one cardiac cycle, thus leading to a total acquisition time of only 5 cardiac cycles.

## Acknowledgment

Y. Zhu and J. Luo were partly supported by the joint project of French ANR 2009 (under ANR-09-BLAN-0372-01) and Chinese NSFC (under 30911130364).

## References

- [1] D. C. Noll, D. G. Nishimura, and A. Macovski, "Homodyne detection in magnetic resonance imaging," *IEEE Transactions on Medical Imaging*, vol. 10, no. 2, pp. 154–163, 1991.
- [2] E. M. Haacke, E. D. Linskog, and W. Lin, "A fast, iterative, partial-fourier technique capable of local phase recovery," *Journal of Magnetic Resonance*, vol. 92, no. 1, pp. 126–145, 1991.
- [3] G. McGibney, M. R. Smith, S. T. Nichols, and A. Crawley, "Quantitative evaluation of several partial Fourier reconstruction algorithms used in MRI," *Magnetic Resonance in Medicine*, vol. 30, no. 1, pp. 51–59, 1993.
- [4] Z. P. Liang and P. C. Lauterbur, *Principles of Magnetic Resonance Imaging: A Signal Processing Perspective*, IEEE Press, New York, NY, USA, 2000.
- [5] P. Margosian, F. Schmitt, and D. Purdy, "Faster MR imaging: imaging with half the data," *Health Care Instrumentation*, vol. 1, no. 6, pp. 195–197, 1986.
- [6] K. P. Pruessmann, M. Weiger, M. B. Scheidegger, and P. Boesiger, "SENSE: sensitivity encoding for fast MRI," *Magnetic Resonance in Medicine*, vol. 42, no. 5, pp. 952–962, 1999.
- [7] M. A. Griswold, P. M. Jakob, R. M. Heidemann, et al., "Generalized autocalibrating partially parallel acquisitions (GRAPPA)," *Magnetic Resonance in Medicine*, vol. 47, no. 6, pp. 1202–1210, 2002.
- [8] D. K. Sodickson and W. J. Manning, "Simultaneous acquisition of spatial harmonics (SMASH): fast imaging with radiofrequency coil arrays," *Magnetic Resonance in Medicine*, vol. 38, no. 4, pp. 591–603, 1997.
- [9] J. J. van Vaals, M. E. Brummer, W. T. Dixon, et al., "'Keyhole' method for accelerating imaging of contrast agent uptake," *Journal of Magnetic Resonance Imaging*, vol. 3, no. 4, pp. 671–675, 1993.
- [10] R. A. Jones, O. Haraldseth, T. B. Muller, P. A. Rinck, and A. N. Oksendal, "K-space substitution: a novel dynamic imaging technique," *Magnetic Resonance in Medicine*, vol. 29, no. 6, pp. 830–834, 1993.
- [11] A. Degenhard, C. Tanner, C. Hayes, D. Hawkes, and M. O. Leach, "Half Fourier acquisition applied to time series of contrast agent uptake," in *Proceedings of the 4th International Conference on Medical Image Computing and Computer Assisted Intervention (MICCAI '01)*, pp. 872–880, Heidelberg, Germany, 2001.
- [12] F. R. Korosec, R. Frayne, T. M. Grist, and C. A. Mistretta, "Time-resolved contrast-enhanced 3D MR angiography," *Magnetic Resonance in Medicine*, vol. 36, no. 3, pp. 345–351, 1996.
- [13] Z.-P. Liang, B. Madore, G. H. Glover, and N. J. Pelc, "Fast algorithms for GS-model-based image reconstruction in data-sharing Fourier imaging," *IEEE Transactions on Medical Imaging*, vol. 22, no. 8, pp. 1026–1030, 2003.
- [14] S. J. Riederer, T. Tasciyan, F. Farzaneh, J. N. Lee, R. C. Wright, and R. J. Herfkens, "MR fluoroscopy: technical feasibility," *Magnetic Resonance in Medicine*, vol. 8, no. 1, pp. 1–15, 1988.
- [15] J. Tsao, "On the UNFOLD method," *Magnetic Resonance in Medicine*, vol. 47, no. 1, pp. 202–207, 2002.
- [16] J. Tsao, P. Boesiger, and K. P. Pruessmann, " $k$ -t BLAST and  $k$ -t SENSE: dynamic MRI with high frame rate exploiting spatiotemporal correlations," *Magnetic Resonance in Medicine*, vol. 50, no. 5, pp. 1031–1042, 2003.
- [17] M. Suga, T. Matsuda, M. Komori, K. Minato, and T. Takahashi, "Keyhole method for high-speed human cardiac cine MR imaging," *Journal of Magnetic Resonance Imaging*, vol. 10, no. 5, pp. 778–783, 1999.
- [18] B. Madore, G. H. Glover, and N. J. Pelc, "Unaliasing by Fourier-encoding the overlaps using the temporal dimension (UNFOLD), applied to cardiac imaging and fMRI," *Magnetic Resonance in Medicine*, vol. 42, no. 5, pp. 813–828, 1999.
- [19] P. Kellman, J. M. Soreger, F. H. Epstein, and E. R. McVeigh, "Low latency temporal filter design for real-time MRI using UNFOLD," *Magnetic Resonance in Medicine*, vol. 44, no. 6, pp. 933–939, 2000.
- [20] B. Hiba, N. Richard, M. Janier, and P. Croisille, "Cardiac and respiratory double self-gated cine MRI in the mouse at 7 T," *Magnetic Resonance in Medicine*, vol. 55, no. 3, pp. 506–513, 2006.